Talanta 186 (2018) 162–168

Contents lists available at ScienceDirect

Talanta

journal homepage: www.elsevier.com/locate/talanta

Determination of C-reactive protein by PAMAM decorated ITO based disposable biosensing system: A new immunosensor design from an old molecule

Münteha Nur Sonuç Karaboğa[a,*], Mustafa Kemal Sezgintürk[b]

[a] Namık Kemal University, School of Health, Tekirdağ, Turkey
[b] Canakkale Onsekiz Mart University, Faculty of Engineering, Bioengineering, Canakkale, Turkey

ARTICLE INFO

Keywords:
11-cyanoundecyltrimethoxysilane
C-reactive protein (CRP)
Biosensor
Electrochemical impedance spectroscopy (EIS)
PAMAM dendrimers

ABSTRACT

This paper demonstrates a new and sensitive electrochemical immunosensor for the analysis of C-reactive protein, an important marker of inflammation. Indium Tin Oxide (ITO) disposable sheets were modified by using 11-cyanoundecyltrimethoxysilane (CUTMS) and PAMAM dendrimers (G:1 amino surfaces) for the first time to immobilize the anti-CRP antibody via covalent interactions. Cyclic voltammetry (CV), and electrochemical impedance spectroscopy (EIS), as well as square wave voltammetry (SWV) methods, were applied to characterize the immobilization stages of anti-CRP and to determine the CRP concentrations. Charge transfer resistance changes were highly linear and sensitive to CRP concentration in the range 21–6148 fg mL^{-1} and were associated with a limit of detection of 0.34 fg mL^{-1}. The system had acceptable repeatability (6.45%, n = 18) and good storage stability (4.5% loss after 6 weeks). Moreover, the binding characterization of CRP to anti-CRP was monitored by a single frequency impedance technique. The amount of CRP in human serum samples was analyzed with a fabricated biosensor to determine the feasibility of the biosensing system for medical purposes. We suggest that 11-CUTMS, a new silanization agent, is ideal for biosensor applications.

1. Introduction

C-reactive protein is an effective plasma protein of hepatic origin that responds to the inflammatory process and has homologues not only in vertebrates but also in many invertebrates. Its plasma concentration increases at an obvious rate during the inflammation process, making it possible to use it for clinical purposes [1,2]. This systemic marker with high clinical susceptibility was the first acute phase protein to be identified. While the average concentration of C reactive protein in healthy individuals is 0.8 mg/L, the serum levels can increase up 10,000-fold rapidly during the development of inflammatory conditions [3]. The most important feature of this protein belonging to the pentraxins family is that it is widely used as a prognostic or diagnostic biomarker especially in cardiovascular disease [4–7], obesity [8,9], diabetes mellitus [10,11], renal diseases [12], some types of cancer [11,13–16] and neurological disorders [17–21]. Currently, CRP analysis in the clinical field is widely performed using turbidimetric, nephelometric techniques or enzyme-linked immunosorbent assay (ELISA) kits. However, these techniques have some disadvantages such as low sensitivity, amount of time involved and high cost [22]. To detect CRP, several methods such as surface plasmon resonance [23,24], chip-based systems [25], optical biosensors [26], quartz crystal microbalance sensors [27,28] and electrochemical sensors [29–31] were developed. Among these, electrochemical techniques become prominent from the point of view of sensitivity, low cost, and practicality.

Poly(amidoamine) (PAMAM) dendrimers consisting of branched monomers can be used effectively in the immobilization process of biorecognition elements thanks to their large surface areas and the high number of functional groups they contain [32]. There are several effective studies in the literature that have used a PAMAM platform for biosensor design [33–36].

ITO-PET electrodes are unique materials in terms of being disposable, cheap, allowing different chemical modifications on the surface, being flexible, and providing reproducible and highly accurate results. Many methods can be used to immobilize the biorecognition element onto the ITO surface. Among these, the most effective and most commonly used method is to use silanization agents such as 3-Glycidoxypropyltrimethoxysilane (3-GOPS) [37], 3-glycidoxypropyltriethoxysilane (3-GOPE) [38] and, 3-aminopropyltriethoxysilane (APTES) [39].

In this study, a new biosensing system was developed to detect CRP, an important biomarker of inflammation. The design of the biosensor

* Corresponding author.
E-mail address: mnsonuc@nku.edu.tr (M.N. Sonuç Karaboğa).

https://doi.org/10.1016/j.talanta.2018.04.051
Received 1 February 2018; Received in revised form 12 April 2018; Accepted 17 April 2018
Available online 19 April 2018
0039-9140/

was planned on the basis of a combination of 11-CUTMS and PAMAM dendrimers. 11-CUTMS is used to form the self-assembled monolayers (SAMs) on the surface, while PAMAM is intended for use as an agent to increase active amino terminals. The immobilization steps of the biosensor were evaluated by cyclic voltammetry (CV), square wave voltammetry (SWV) and electrochemical impedance spectroscopy (EIS). The developed biosensor surface morphology was visualized by scanning electron microscopy (SEM). In order to achieve a biosensor system with a high applicability, extensive optimization studies were carried out. Repeatability, reproducibility and selectivity studies were also completed. The kinetic behavior of the bond between anti-CRP and CRP was followed effectively by an electrochemical technique called single frequency impedance. Analysis of the concentration of CRP in blood serum samples with the developed biosensor and comparison of the results with reference methods were the end points of this study.

2. Materials and methods

2.1. Chemicals and apparatus

The reference electrode and counter electrode were purchased from BASi (West Lafayette, IN, USA), disposable ITO-coated PET films (The transmittance and surface resistivity are 550 nm (> 79%) and 60 Ω/square, respectively and geometry area 0.25 cm^2) Standard anti-CRP and CRP antigen were acquired from Sigma Aldrich (St. Louris, MO, USA) CRP, anti-CRP portions were prepared at certain concentrations in 50 mM pH 7.0 phosphate buffer and stored at −20 °C. until use. 11-cyanoundecyltrimethoxysilane was purchased from abcr GmbH&Co. (Karlsruhe, Germany). Amino surfaces PAMAM (generation:1), and the other reagants were supplied from Sigma Aldrich (St. Louris, MO, USA). Ultrapure water (18.2 MΩ/cm) was obtained from a Elga LC134 system and used throughout.

All electrochemical experiments were carried out in an electrochemical cell (three electrode system), consist of a sheet of ITO film as a working electrode, a platinum wire as a counter electrode and a silver/silver chloride as a reference electrode which has a volume of 10 mL 1 M KCl, 5 mM $[Fe(CN)_6]^{4-}$ and 5 mM $[Fe(CN)_6]^{3-}$ redox probe. The blood samples were obtained by research ethics committee approval with the number of 2013/86/07/05 from Namık Kemal University, Faculty of Medicine. All the electrochemical measurements, including electrochemical impedance spectroscopy, were performed by a Potentiostat/Galvanostat (Gamry Interface 1000 Gamry Instruments, Warminster, USA). The measurements were checked by a personal computer running the electrochemical software program of Gamry Instruments (Echem Analyst) for data collection, monitoring of optimization parameters, and processing.

2.2. Preparation of ITO-based electrodes

The first step in the design of the biosensor is the cleaning of the ITO electrodes. The ITO-PET electrodes were polished by sonicating with acetone, soap solution and ultrapure water respectively for 10 min. Before proceeding further, all the electrodes were gently dried under ultra-pure argon gas. In order to construct the silanization agent on the ITO electrodes, hydroxide groups must first be formed on the surface of each cleaned electrode. For this, the electrodes were incubated at room temperature for 90 min in a solution containing hydrogen peroxide, ammonium hydroxide and ultrapure water (1:1:5). The hydroxyl-group-formed electrodes were gently washed with ultrapure water and dried with ultrapure argon gas.

2.3. Fabrication of immunosensor

After cleaning procedure and hydroxyl group formation on the surface, the ITO electrodes were immersed into 0.5% 11-CUTMS solution prepared in pure toluene-ethanol mixture and allowed to incubate overnight at room temperature. Then, in order to remove the physically adsorbed 11-CUTMS molecules, the electrodes were washed with ultra pure water and gently dried with ultra pure argon gas. In the next step, the ITO-based electrodes were immersed in the 1.0% PAMAM solution prepared in methanol and allowed to incubate for 60 min at room temperature. PAMAM-modified electrodes were washed with ultrapure water and dried again with argon gas. Afterwards, PAMAM-modified electrodes were immersed in 1% pH 7.0 PBS solution of glutaraldehyde, a cross-linker commonly used in the activation of amino groups, and allowed to incubate for 15 min. ITO substrates modified with 11-CUTMS and PAMAM were dried with argon gas gently and immersed into 100 µL of 63.4 ng mL^{-1} anti-CRP solution in a dark and moist medium as quickly as possible for 60 min. After incubation with anti-CRP antibody, electrodes were washed with ultra-pure water to remove unbound antibody molecules. Finally, anti-CRP antibody-immobilized ITO electrodes were treated with BSA (0.5%) for 60 min to block the active ends. At the end of this, the electrodes were washed with ultrapure water and gently dried with ultra pure argon gas. With this last step, the now-prepared biosensor was stored at +4 °C until the CRP measurements were performed. The bare (cleaned) and modified ITO substrates are indicated as ITO, ITO-OH, ITO/CUTMS, ITO/CUTMS/antiCRP, ITO/CUTMS/anti-CRP/BSA and ITO/CUTMS/antiCRP/BSA/CRP, respectively.

2.4. Electrochemical measurements

Immobilization steps, optimization assays and analytical properties of the developed biosensor were monitored with electrochemical impedance spectroscopy (EIS), cyclic voltammetry (CV), and square wave voltammetry (SWV).

All electrochemical experiments were carried out in a solution containing 5 mM K3[Fe(CN)6]/K4[Fe(CN)6] (1:1) as a redox probe. The redox probe solution also contained 0.1 M KCl to decrease the resistance of probe solution.

In cyclic voltammetry experiments, the potential was differentiated between −500 mV and 1000 mV (step size: 10 mV, scan rate: 100 mV/s). Electrochemical impedance measurements were performed by applying an alternating potential of 5 mV to the working electrode. The formal potential applied in the impedance studies was 0 V. Another important parameter in impedance measurements was the frequency range from 50,000 to 0.05 Hz. SWV were carried out with potential scan range: 0–1.2 V, and pulse size: 25 mV.

Morphological observation of the different surfaces obtained during the fabrication process of the biosensor used a field emission scanning electron microscope (FEI-Quanta FEG 250) operated at the Scientific and Technological Research Center of Namık Kemal University (NABILTEM). 5 kV was used as an acceleration voltage to obtain SEM images.

2.5. Measurement principle of C-reactive protein

Each of the 11-CUTMS and PAMAM-modified ITO-based biosensors were incubated with standard CRP solutions prepared at different concentrations for 60 min at room temperature and in darkness. After the incubation period, the biosensor was gently immersed into ultrapure water to remove physically adsorbed CRP molecules. Electrochemical impedance spectroscopy and cyclic voltammetry measurements of each CRP concentration were performed by immersing the working electrodes into the redox probe. EIS and CV measurements were recorded via EChem Analyst software program.

K3 [Fe (CN) 6] / K4 [Fe (CN) 6] is a redox couple that acts as an electrochemical mediator between the biological element and the surface of the modified electrode.

In electrochemical impedance spectroscopy, charge transfer resistance (Rct) is a demonstration of two effects: (1) potential energy associated with the oxidation or reduction event at the electrode. (2) the formation of an electrostatic repulsion or steric barrier with the

energy barrier of the redox species reaching the electrode [40].

3. Results and discussion

3.1. Immobilization of anti-CRP

Silane chemistry is frequently used in the design of ITO-based biosensors. While the 11- cyanoundecyltrimethoxysilane coupling agent gives a condensation reaction to form a mono layer, it simultaneously interacts with ITO substrates through the -OH groups on the surface.

Organo-functional silanes may have high reactivity to different surfaces due to their low surface tension. They may form interactions and an adequate transition interphase between the monolayer and the substrate to be bonded. 11- cyanoundecyltrimethoxysilane is one of the most useful organosilanes that can be used in the immobilization step. The cyano group with an unshared electron pair in the nitrile nitrogen can form intermolecular bonds with the appropriate hydrogen donor sample molecules. In addition, 11-CUTMS containing more carbon-chain than other silane agents allows a more compact stack of SAM to be formed. To form a stable monolayer on the surface, incubation was performed overnight with 11-CUTMS. After the self-assembled monolayer was generated on the surface by 11-CUTMS, the electrodes were immersed in PAMAM solution. At this point the use of the PAMAM solution is intended to increase anti-CRP immobilization performance by increasing the active amino terminals. After the electrodes were treated with the PAMAM solution, anti-CRP immobilization was performed in the medium with glutaraldehyde used as the crosslinker. If there were functional open ends after immobilization, BSA was used as blocking agent. All of these steps are summarized in Graphical Abstract.

The step-by-step formation of the constructed biosensor was monitored by EIS and CV techniques. $K_3[Fe(CN)_6]/K_4[Fe(CN)_6]$ is a redox couple including a redox reaction between the biological material and modified electrode surface as an electrochemical mediator.

Changes in the relationship between the biorecognition element and the analyte during the biosensor design lead to differences in the capacitance and resistance properties of the conducting or semiconducting surface. All these changes are effectively reflected in electrochemical impedance spectroscopy results. In this regard, EIS is an effective electrochemical method used for the surface phenomena of the biorecognition element and in the determination of biosensing material. The impedance spectra for each immobilization step of anti-CRP are shown in Fig. 1A and on CV voltammograms in Fig. 1B

The semicircle diameter in an impedance spectrum indicates the electron transfer resistance; R_{ct}. Electron-transfer kinetics of the redox probe at the electrode-solution interface are controlled by electron transfer resistance. The charge transfer resistance (Rct) value of bare ITO was assessed as 39,110 Ω. As seen from impedance spectra, the formation of –OH groups on the ITO surface causes more conductive behavior toward the electrode proven by a decrease in charge transfer resistance (1737 Ω). After the SAM of 11-CUTMS was formed on the surface, the long aliphatic chain portion of the structure was stacked tightly, resulting in effective hydrophobic interactions. In addition to this, negatively charged -CN groups in 11-CUTMS push the redox probe, making it difficult to diffuse to the surface. These effects were reflected as an obvious increase in the charge transfer resistance on the EIS results (2360 Ω). In the next step, amino surface PAMAM dendrimers were attached to the modified surface through chemical covalent bonding by the reaction between the cyano group and the primary amino groups of dendrimers, with the structure of a secondary ketimine formed. As expected, electrostatic attraction between the positive amino groups on PAMAM and the negatively-charged redox probe is reflected in the impedance spectra as a decrease in Rct value (1104 Ω). The glutaraldehyde was used as a crosslinker between the antibody and the primary amino groups of PAMAM in the immobilization step of the anti-CRP onto ITO surface. Covalent immobilization of anti-CRP on the electrode surface has obviously increased the insulating property of the surface resulting in a clear increase in charge transfer resistance (2590 Ω) as seen from Fig. 1A. The PAMAM dendrimer makes the surface of the immunosensor less negative due to its positive surface charges, thus allowing the redox couple to come closer to the sensor surface so that the charge transfer is more effective. This result demonstrates that the platform composed of 11-CUTMS and PAMAM dendrimers allows better immobilization of anti-CRP. Likewise, BSA used for blocking active amino ends also has the effect of enhancing the electron resistance on the surface (3000 Ω).

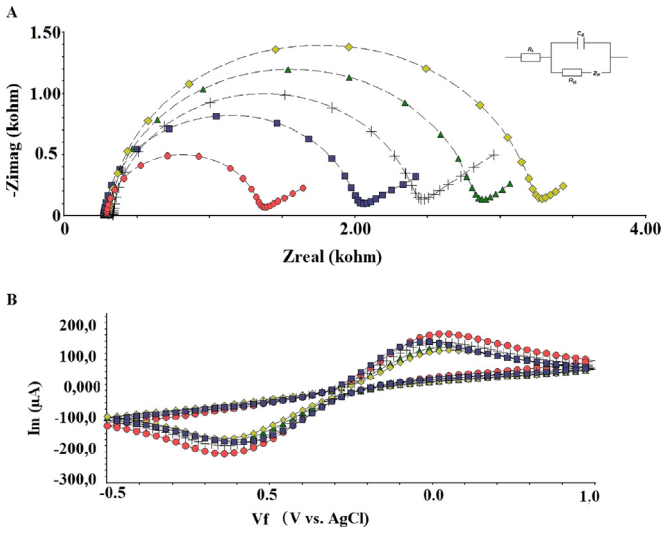

Fig. 1. EIS spectrum (A) and cyclic voltammogram (B) of immobilization steps. Pink (-•-•-): ITO/OH/11-CUTMS/PAMAM, blue (-■-■-): ITO/OH, (-+-+-): ITO/OH/11-CUTMS, green (-▲-▲-): ITO/OH/11-CUTMS/PAMAM/anti-CRP, yellow (-◆-◆-): ITO/OH/11-CUTMS/PAMAM/anti-CRP/BSA. (For interpretation of the references to color in this figure legend, the reader is referred to the web version of this article.)

Cyclic voltammograms were also applied to investigate the electrochemical behavior of the anti-CRP-based biosensing system. The impedance spectra and cyclic voltammogram results are compatible with each other. After the self-assembled mono layer was formed with 11-CUTMS, the negatively-charged cyano groups and negatively-charged redox probes repelled each other, causing the peak current signal to decrease. As seen from Fig. 1B, when CUTMS-modified electrodes were treated with PAMAM, the electrostatic attraction between the primary amino groups of the PAMAM structure and the redox probe caused the peak currents to increase. After the covalent immobilization of anti-CRP onto the CUTMS-modified ITO surface there was a decrease in both anodic and cathodic peaks due to preventive effects of the immobilized layers between the redox probe and electrode surface.

3.2. Optimization studies for the CRP biosensor

The activity of the immunosensors developed on the basis of the affinity between the antigen and the antibody is highly dependent on the conditions involved in forming the electrode surface and the electrical charge on the surface. Therefore, it is possible to understand the capacitance variations of bioaffinity complex formation by determining optimal conditions.

PAMAM dendrimers are composed of numerous primary amino groups which favor the anchoring of more anti-CRP on the sensing surface. Optimizing the concentration of PAMAM allows for better anti-CRP immobilization and optimal recognition of CRP. For this purpose, different concentrations of PAMAM (0.5%, 1%, 1.5% 2% in ethanol) were applied on ITO electrodes modified with 1% 11-CUTMS for 60 min at room temperature. As seen from calibration curves (Supplemental data, Fig. 1S) obtained from EIS data, while PAMAM of 2.0% has a

relatively low charge transfer resistance and a very low coefficient of determination (R^2:0.7633), 0.5% PAMAM has high charge transfer resistance and a relatively low coefficient of determination (R^2:0.8212). However, results for 1.0% showed high charge transfer resistance and high coefficient of determination (R^2:0.9412). The results show that as the PAMAM concentration increases, the formation of an insulating layer on the surface increases and this layer may cause irregularity in the immobilization of anti-CRP. Thus, 1.0% PAMAM was chosen for 11-CUTMS-based PAMAM-modified biosensing system for optimal immunological recognition of the designed biosensor.

In the last step of the optimization studies, the effect of the anti-CRP concentration on the biosensing system response was investigated. For this aim, biosensors were prepared with different concentrations of anti-CRP (63.4 ng/mL, 634 ng/mL and 6.34 μg/mL) for 60 min at room temperature. At higher antibody concentrations, a decrease in sensitivity of the immunosensor was observed (for 6.34 μg/mL and 634 ng/mL of anti-CRP R^2 = 0.9112 and 0.9267 respectively). This may be due to the fact that the CRP may not easily diffuse to the surface due to the high steric hindrance that occurs and that the possible protein-protein interactions reduce the detection of CRP. When the calibration curves obtained from the EIS data were analyzed (Fig. 2S), anti-CRP solution of 63.4 ng mL^{-1} was optimized for optimal recognition of CRP.

3.3. Analytical characteristics of designed biosensing system

Standard CRP solutions prepared under optimal conditions and at different concentrations were applied to the developed biosensing system to evaluate the analytical performance of the system. The relationship between antibody concentration and electron transfer resistance was determined by the equivalent circuit model inserted in Fig. 1A. This equivalent circuit model, which is frequently used in impedimetric biosensing systems, is composed of resistive and capacitive elements as well as the Warburg element. *Rct* is the charge transfer resistance, *Rst* indicates resistance of the working solution of system, CPE indicates the constant phase element of the bioactive layer and Z_w is the Warburg element. The most obvious variance among these elements is the charge transfer resistance (Rct). This circuit was applied to characterize electron transfer from an electrolyte to the electrode surface. Based on this information, the calibration graph of the CRP immunosensor was drawn using the following equation.

$$\Delta R_{ct} = R_{ct}(CRP) - R_{ct}(BSA)$$

where $R_{ct(CRP)}$ is the value of electron transfer resistance after antibody-antigen binding between anti-CRP and CRP. Rct(BSA) is the value of the semicircle diameter of the blocking step for the constructed biosensor with BSA. Nyquist plots and cyclic voltammograms of the fabricated biosensor incubated in increasing concentrations of CRP are presented in Fig. 2A and B. As the CRP concentration increased, a linear increase in the diameter of the semicircle on Nyquist plots was observed. This increase in Rct may be due to the fact that the antibody-antigen complex formed on the biosensor surface reduces the conductivity of the system. Similarly, Fig. 2B illustrates that as the CRP concentration increases peak currents of CV were also reduced. This is because the immunocomplex growing on the biosensing surface enhanced the electron transfer barrier significantly due to the increase of the CRP concentrations. The calibration curve (Fig. 2C) showed a linear correlation in the range from 21 to 6148 fg mL^{-1}. Each of the prepared ITO electrodes is disposable. A single electrode was used for each CRP concentration (8 different concentrations ranging from 21 fg.mL^{-1} to 6148 fg.mL^{-1}). LOD (limit of detection) and LOQ (limit of quantification) values were determining according the IUPAC recommendations [41] as 0.34 fg. mL^{-1} and 1.13 fg mL^{-1} respectively. These results emphasize that the developed biosensor shows high sensitivity for CRP assay.

Square wave voltammetry is widely used in the development of biosensors for rapid detection of disease-associated biomarkers, thanks

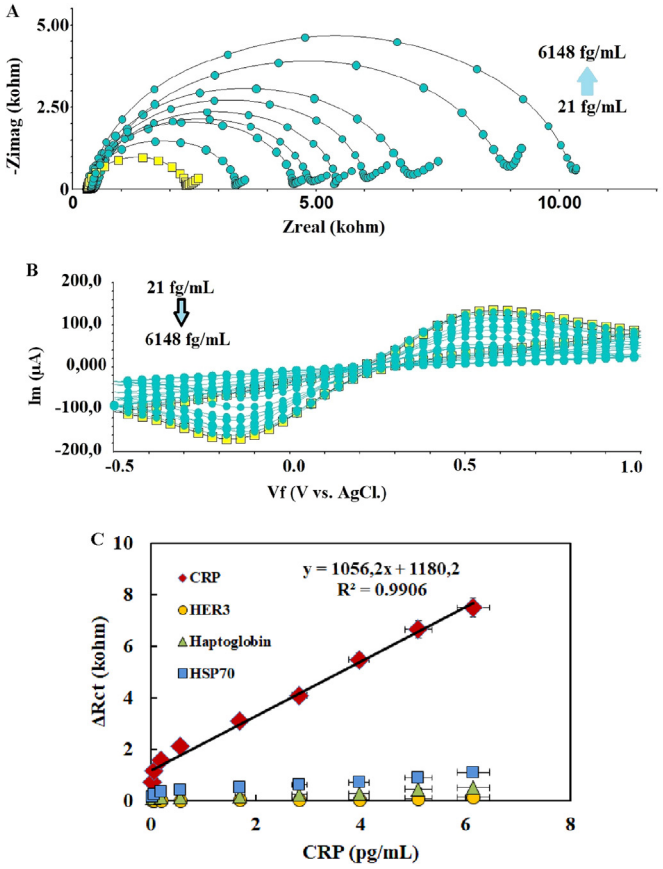

Fig. 2. Impedance spectra (A), cyclic voltammograms (B) obtained for different concentrations of CRP. **(C)** Concentration-dependent calibration curve for CRP obtained by the biosensor based on anti-CRP at optimal working conditions. (-■-■-): ITO/OH/CUTMS/antiCRP/BSA(-•-•-): ITO/OH/CUTMS/antiCRP/BSA/CRP.

to the high selectivity and sensitivity that it possesses. This method changes the potential of the sample by pulsing to another, with a potential for sweeping the changing potentials. The reason for frequent use of SWV is the ability to operate at high frequencies [42]. This means that SWV experiments can be performed very quickly and that electroactive species can be protected with respect to other pulse techniques. Therefore, there is a linear relationship between the decrease in peak current as the CRP concentration increases (Fig. 3A). As seen from the calibration chart (inserted in Fig. 3B), the SWV results have similar sensitivities with EIS. The advantage of SWV over EIS is that the potential scan is completed within a few seconds whereas a longer period is needed for EIS.

The repeatability of ITO biosensor was determined by analysis of

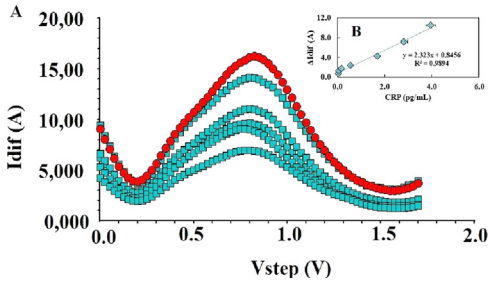

Fig. 3. A. Square Wave Voltammograms obtained for different concentrations of CRP, and CRP calibration curve obtained by the present biosensor. (-•-•-): ITO/OH/CUTMS/antiCRP/BSA; (-■-■-): ITO/OH/CUTMS/antiCRP/BSA/CRP. **B.** Calibration curve for CRP obtained by SWV.

the same concentration of CRP (1.7 pg/mL) with 18 electrodes prepared under similar conditions. It was found that the immunosensor had excellent repeatability bearing in mind that the correlation coefficient of the analysis was 6.45% and the average value and standard deviation were calculated as 1.86 and 0.12 pg/mL.

The reproducibility of ITO-based CRP immunosensor was evaluated by monitoring the responses of 10 biosensor systems prepared with the same procedure in the 21–6148 fg/mL determination range. The responses of these immunosensors were found to represent similar linearity in the range between 21 and 6148 fg mL^{-1} for CRP. The relative standard deviations were also calculated by using the slopes and the intercepts of the linear equations obtained from these 5.35% and 12.39%. Results of reproducibility and repeatability demonstrate that the surface platform composed of PAMAM and 11-CUTMS allows high sensitivity recognition of CRP in the range of concentrations from 21 to 6148 fg/mL (Table 1S).

The storage stability of the fabricated ITO-based disposable biosensor was specified by monitoring the impedimetric response of the immunosensor at the end of specific periods. Immunosensors prepared under optimal conditions were stored at 4 °C and CRP detection was performed in every 7 day period. For the first six weeks, immunosensors almost completely retained their initial activity (95.5%), whereas at the end of the seventh week the immunosensor response reduced significantly due to some destructive effects and non-specific bindings.

3.4. Single frequency impedance (SFI) experiments

One of the effective electrochemical methods for monitoring the kinetic behavior of antibody/antigen binding is single frequency impedance. This method is useful to better understand alteration on the electrical surface. For this purpose, the potentiostat was set up at a fixed frequency of 10 Hz which was defined with the assistance of Bode plots. While the Bode plots provide important information about the frequency of the system, the Nyquist plot is weak on this point. The variation in impedance value was measured at the fixed frequency as a function of time and phase angle for 30 min. In Fig. 4, time-dependent change in impedance is presented by a blue curve while the change in the phase angle as a function of time is shown by the pink curve. When the CRP interacts with its target anti-CRP, an extra hindrance effect occurs on the designed surface and this is reflected as a decrease in phase angle and an increase in impedance value of the circuit. The advantage of this method is to characterize surface events such as affinity of immunocomplex through a time-dependent system. However, single frequency impedance is strongly affected by environmental factors like electromagnetic waves.

3.5. Selectivity

The selectivity of the constructed biosensor towards target CRP was investigated by monitoring ΔRct of the biosensor for a nonspecific interaction, if any, with the nonspecific protein antigens of human HER-3, heat shock protein (HSP70) and haptoglobin over the same concentration range of 21–6148 fg / mL. Fig. 2C shows that the non specific of HER-3 to the biosensor has a very small contribution. However, the interest of haptoglobin and HSP70 in the developed biosensor is slightly higher than HER3. This negligible contribution of the nonspecific interactions to the total Rct response represents good selectivity of the biosensor to the specific target CRP.

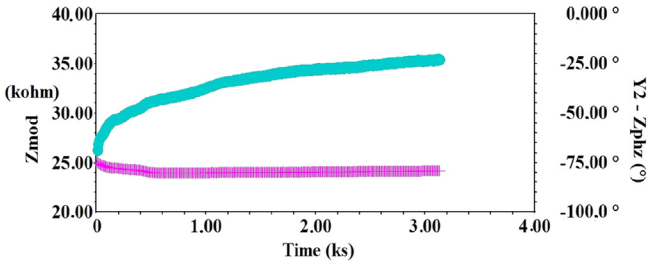

Fig. 4. Single frequency impedance measurement of biosensor based on CRP (■ variation is phase angle; pink • variation is impedance; blue). (For interpretation of the references to color in this figure legend, the reader is referred to the web version of this article.)

Table 1
The results for the sample analysis and comparison of methods used for CRP.

Samples	Clinical results from NKU hospital[a] (mg/L)	Found by biosensor (mg/L)	Relative Differences	Recovery (%)
1	0.9	0.83	7.77	92.23
2	0.5	0.61	22	122
3	2.5	2.92	16.8	116.8
4	0.9	1.22	35.5	135.5
5	1.3	1.11	14.61	85.39
6	2.7	2.56	5.18	94.82
7	1.2	1.05	12.5	87.5
8	0.7	0.82	17.14	117.14

[a] obtained from the reference methods used in the Namık Kemal University hospital.

3.6. Application of immunosensor for CRP detection in clinical serum samples

The fabricated immunosensor was used for detection of CRP in eight human serum samples containing different concentrations of CRP. Human serum samples were first diluted 10^6 times with pH 7.0 PBS because the CRP content of serum from a healthy person has higher concentration than the proposed biosensor detection range. The serum samples were randomly collected from Namık Kemal University Hospital, Faculty of Medicine with research ethics committee approval number 2013/86/07/05. The results for the use of the constructed biosensor for CRP detection are compared with serum CRP levels determined at the hospital with a reference technique (Table 1). As seen from the results, good agreement and accuracy was observed between the reference method of the Medical Faculty Hospital and the proposed immunosensor.

As shown in Table 2, studies of the biosensor system for identification of CRP are very limited, even though CRP is a very important inflammatory biomarker and frequently referenced parameter in the medical field. Nevertheless, many of studies reported in the literature have high cost and low sensitivity for CRP. 11-CUTMS is a relatively new material that has not previously been applied in biosensor strategies. Moreover, this useful organosilane has a perfect harmony with PAMAM, making the determination range of CRP very wide. The LOD value of the developed biosensor system and its sensitivity in serum samples are promising.

3.7. Morphological analysis by SEM

The chemical and physical changes on the surface can be monitored morphologically step by step with scanning electron microscopy. Tracing these changes provides superior information about the biosensor's motion. The SEM images for the constructed biosensor are shown in Fig. 5. Morphological change in the surface after modification with SAM of 11-CUTMS is shown in Fig. 5A. Fig. 5B shows the image after PAMAM modification. PAMAM molecules appear to be spheres with submicron dimensions. Fig. 5C shows the globular structure of anti-CRP molecules covalently linked to PAMAM molecules. After blocking the active groups on the surface with BSA, the changes in the morphology of the surface are shown in Fig. 5D. The biosensor surface

Table 2
Comparison of analytical characteristics of electrochemical based CRP biosensor reported in literature.

Electrode configuration	Immobilization method	Linear detection range for CRP	Measurement Principle	LOD	References
HS-C11-(EG)3-OCH2-COOH SAMs on gold electrode	EDC-NHS[a] chemistry	0.5–50 nM	EIS and CV	176 ± 18 p.M.	[22]
Carbon nanofiber	PMMA[b]	0.05–5 μg/mL	EIS and CV	11 ng/mL	[43]
rGO-AuNP modified ITO elektrode	MPA[c]	1 ng/mL^{-1} μg/mL	EIS and CV	0.08 ng/mL	[31]
rGO modified SPCE	PyNHS[d]	10 ng/mL^{-10} μg/mL	SFI	0.1 ng/mL	[44]
Ni-modified Au nanoparticle	Cysteine SAMs	10^{-7} g·mL^{-1} 10^{-6} g·mL^{-1}	EIS and CV	3.56×10^{-9} g·mL^{-1}	[45]
DNA attached to Au	DNA adsorbtion	3.125–25 mg/L	EIS and CV	–	[46]
SPE-gold nanoparticle	Adsorbtion	0.047–23.6 μg/mL^{-1}	CV	17 ng mL^{-1}	[47]
ITO-PET elektrode	SAMs with CPTMS[e]	3.25–208 fg/mL	EIS and CV	0.455 fg/mL	[48]
ITO-PET elektrode	CUTMS SAMs and PAMAM	21–6148 fg/mL	EIS and CV	0.34 fg/mL	present

[a] EDC-NHS: 1-ethyl-3-(3-dimethylaminopropyl) carbodiimide and N-hydroxysuccinimide.
[b] PMMA: poly(methyl methacrylate).
[c] MPA: 3-mercaptopropionic acid.
[d] PyNHS: 1-pyrenebutyric acid *N*-hydroxy succinimide.
[e] CPTMS: cyanopropyltrimethoxysilane.

was once again changed after being treated with CRP. The bean-like structures shown in Fig. 5E may be attributed to the interaction of anti-CRP and CRP on the PAMAM modified electrode surface.

4. Conclusion

In this study, a novel, low cost, easily prepared disposable biosensing system for the determination of CRP, an important marker of

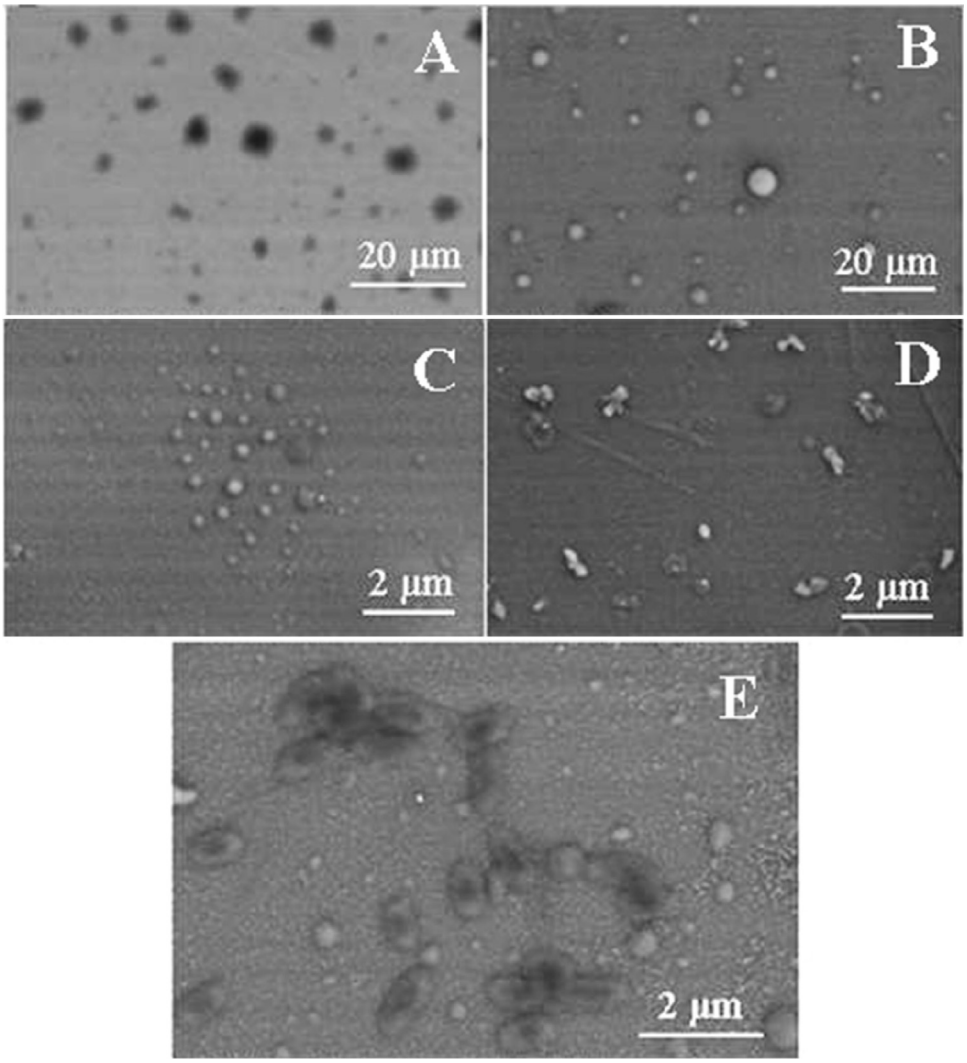

Fig. 5. SEM images related with the morphological changes of the biosensor surfaces. [(A) ITO/11-CUTMS; (B) ITO/11-CUTMS/PAMAM; (C) ITO/11-CUTMS/PAMAM/anti-CRP; (D) ITO/11-CUTMS/PAMAM/anti-CRP/BSA; (E) ITO/11-CUTMS/PAMAM/anti-CRP/BSA/CRP.

inflammation, was successfully developed. The sensing platform composed of 11-CUTMS and PAMAM molecules for the development of this biosensor is very new and has been used for the first time. In particular, no studies have been found in the scientific literature on the use of 11-CUTMS in biosensor systems. This shows the superiority of this study in terms of innovation. 11-CUTMS, a silanization agent, was well-coordinated with ITO-PET substrate while being modified with PAMAM to play a role in the precise and effective determination of CRP. The primary amino groups present in PAMAM have been implicated in the detection range of CRP at 21–6148 fg/mL, ensuring successful immobilization of anti-CRP on the surface. Moreover, 11-CUTMS and PAMAM-based biosensing system allowed reproducible and repeatable analysis of CRP with impressive LOD (0.34 fg. mL^{-1}) and LOQ (1.13 fg mL^{-1}) values.

CRP levels in human serum sample experiments showed good agreement with the reference method, though 11-CUTMS and PAMAM-modified disposable ITO material should prevent undesirable physical bonding to the electroactive surface and provide selective results for CRP. Moreover, the lifetime of the fabricated biosensor is relatively long, which is an important parameter for future prospective studies in the medical field. Finally, it is proposed that 11-CUTMS is a very new silanization agent and combined with PAMAM could be used in biosensor construction processes due to its excellent suitability for ITO substrates.

Appendix A. Supporting information

Supplementary data associated with this article can be found in the online version at http://dx.doi.org/10.1016/j.talanta.2018.04.051.

References

[1] S. Black, I. Kushner, D. Samols, C-reactive protein, J. Biol. Chem. 279 (2004) 48487–48490.
[2] R. Schulz, G. Heusch, C-reactive protein, Hypertension 57 (2011) 151–153.
[3] G. Hirschfield, M. Pepys, C-reactive protein and cardiovascular disease: new insights from an old molecule, Qjm 96 (2003) 793–807.
[4] E.R.F. Collaboration, C-reactive protein, fibrinogen, and cardiovascular disease prediction, N. Engl. J. Med. 2012 (2012) 1310–1320.
[5] J. Genest, C-reactive protein: risk factor, biomarker and/or therapeutic target? Can. J. Cardiol. 26 (2010) 41A–44A.
[6] P.M. Ridker, Inflammation, C-reactive protein, and cardiovascular disease, Am. Heart Assoc. (2014).
[7] P.M. Ridker, N. Rifai, L. Rose, J.E. Buring, N.R. Cook, Comparison of C-reactive protein and low-density lipoprotein cholesterol levels in the prediction of first cardiovascular events, N. Engl. J. Med. 347 (2002) 1557–1565.
[8] M. Letizia Hribal, T. Vanessa Fiorentino, G. Sesti, Role of C reactive protein (CRP) in leptin resistance, Curr. Pharm. Des. 20 (2014) 609–615.
[9] A. Pires, P. Martins, A.M. Pereira, J. Marinho, P.V. Silva, M. Marques, E. Castela, C. Sena, R. Seiça, Pro-inflammatory triggers in childhood obesity: correlation between leptin, adiponectin and high-sensitivity C-reactive protein in a group of obese Portuguese children, Rev. Port. Cardiologia 33 (2014) 691–697.
[10] Z. Al-Hamodi, A.-H. Molham, A. Al-Meeri, R. Saif-Ali, Association of adipokines, leptin/adiponectin ratio and C-reactive protein with obesity and type 2 diabetes mellitus, Diabetol. Metab. Syndr. 6 (2014) 99.
[11] C. Schalkwijk, D. Poland, W. Van Dijk, A. Kok, J. Emeis, A. Dräger, A. Doni, V. Van Hinsbergh, C. Stehouwer, Plasma concentration of C-reactive protein is increased in type I diabetic patients without clinical macroangiopathy and correlates with markers of endothelial dysfunction: evidence for chronic inflammation, Diabetologia 42 (1999) 351–357.
[12] B.T. Lee, F.A. Ahmed, L.L. Hamm, F.J. Teran, C.-S. Chen, Y. Liu, K. Shah, N. Rifai, V. Batuman, E.E. Simon, Association of C-reactive protein, tumor necrosis factor-alpha, and interleukin-6 with chronic kidney disease, BMC Nephrol. 16 (2015) 77.
[13] K.H. Allin, B.G. Nordestgaard, Elevated C-reactive protein in the diagnosis, prognosis, and cause of cancer, Crit. Rev. Clin. Lab. Sci. 48 (2011) 155–170.
[14] S. Hong, Y. Kang, B.C. Cho, D.J. Kim, Elevated serum C-reactive protein as a prognostic marker in small cell lung cancer, Yonsei Med. J. 53 (2012) 111–117.
[15] P.I. Karakiewicz, G.C. Hutterer, Q.D. Trinh, C. Jeldres, P. Perrotte, A. Gallina, J. Tostain, J.J. Patard, C-reactive protein is an informative predictor of renal cell carcinoma-specific mortality, Cancer 110 (2007) 1241–1247.
[16] M. Martino, T. Klatte, C. Seemann, M. Waldert, A. Haitel, G. Schatzl, M. Remzi, P. Weibl, Validation of serum C-reactive protein (CRP) as an independent prognostic factor for disease-free survival in patients with localised renal cell carcinoma (RCC), BJU Int. 111 (2013).
[17] K. Henriksen, S.E. O'Bryant, H. Hampel, J.Q. Trojanowski, T.J. Montine, A. Jeromin, K. Blennow, A. Lönneborg, T. Wyss-Coray, H. Soares, The future of blood-based biomarkers for Alzheimer's disease, Alzheimer'S. Dement. 10 (2014) 115–131.
[18] P. Komulainen, T.A. Lakka, M. Kivipelto, M. Hassinen, I.M. Penttilä, E.-L. Helkala, H. Gylling, A. Nissinen, R. Rauramaa, Serum high sensitivity C-reactive protein and cognitive function in elderly women, Age Ageing 36 (2007) 443–448.
[19] P.L. McGeer, E.G. McGeer, Inflammation and neurodegeneration in Parkinson's disease, Park. Relat. Disord. 10 (2004) S3–S7.
[20] K. Nilsson, L. Gustafson, B. Hultberg, C-reactive protein level is decreased in patients with Alzheimer's disease and related to cognitive function and survival time, Clin. Biochem. 44 (2011) 1205–1208.
[21] M. Yarchoan, N. Louneva, S.X. Xie, F.J. Swenson, W. Hu, H. Soares, J.Q. Trojanowski, V.M.-Y. Lee, M.A. Kling, L.M. Shaw, Association of plasma C-reactive protein levels with the diagnosis of Alzheimer's disease, J. Neurol. Sci. 333 (2013) 9–12.
[22] T. Bryan, X. Luo, P.R. Bueno, J.J. Davis, An optimised electrochemical biosensor for the label-free detection of C-reactive protein in blood, Biosens. Bioelectron. 39 (2013) 94–98.
[23] S.A. Vance, M.G. Sandros, Zeptomole detection of C-reactive protein in serum by a nanoparticle amplified surface plasmon resonance imaging aptasensor, Sci. Rep. 4 (2014).
[24] H.-C. Kim, S.-K. Lee, W.B. Jeon, H.-K. Lyu, S.W. Lee, S.W. Jeong, Detection of C-reactive protein on a functional poly (thiophene) self-assembled monolayer using surface plasmon resonance, Ultramicroscopy 108 (2008) 1379–1383.
[25] C.-H. Kim, J.-H. Ahn, J.-Y. Kim, J.-M. Choi, K.-C. Lim, T.J. Park, N.S. Heo, H.G. Lee, J.-W. Kim, Y.-K. Choi, CRP detection from serum for chip-based point-of-care testing system, Biosens. Bioelectron. 41 (2013) 322–327.
[26] B.B. Kim, W.J. Im, J.Y. Byun, H.M. Kim, M.-G. Kim, Y.-B. Shin, Label-free, CRP detection using optical biosensor with one-step immobilization of antibody on nitrocellulose membrane, Sens. Actuators B: Chem. 190 (2014) 243–248.
[27] P. Ding, R. Liu, S. Liu, X. Mao, R. Hu, G. Li, Reusable gold nanoparticle enhanced QCM immunosensor for detecting C-reactive protein, Sens. Actuators B: Chem. 188 (2013) 1277–1283.
[28] N. Kim, D.-K. Kim, Y.-J. Cho, Development of indirect-competitive quartz crystal microbalance immunosensor for C-reactive protein, Sens. Actuators B: Chem. 143 (2009) 444–448.
[29] J. Wang, J. Guo, J. Zhang, W. Zhang, Y. Zhang, RNA aptamer-based electrochemical aptasensor for C-reactive protein detection using functionalized silica microspheres as immunoprobes, Biosens. Bioelectron. 95 (2017) 100–105.
[30] X. Bing, G. Wang, Label free C-reactive protein detection based on an electrochemical sensor for clinical application, Int. J. Electrochem. Sci. 12 (2017) 6304–6314.
[31] A.K. Yagati, J.-C. Pyun, J. Min, S. Cho, Label-free and direct detection of C-reactive protein using reduced graphene oxide-nanoparticle hybrid impedimetric sensor, Bioelectrochemistry 107 (2016) 37–44.
[32] E.B. Bahadır, M.K. Sezgintürk, Poly (amidoamine)(PAMAM): an emerging material for electrochemical bio (sensing) applications, Talanta 148 (2016) 427–438.
[33] Z.-M. Liu, Y. Yang, H. Wang, Y.-L. Liu, G.-L. Shen, R.-Q. Yu, A hydrogen peroxide biosensor based on nano-Au/PAMAM dendrimer/cystamine modified gold electrode, Sens. Actuators B: Chem. 106 (2005) 394–400.
[34] G. Castillo, K. Spinella, A. Poturnayová, M. Šnejdárková, L. Mosiello, T. Hianik, Detection of aflatoxin B 1 by aptamer-based biosensor using PAMAM dendrimers as immobilization platform, Food Control 52 (2015) 9–18.
[35] M.K. Sezgintürk, Z.O. Uygun, An impedimetric vascular endothelial growth factor biosensor-based PAMAM/cysteamine-modified gold electrode for monitoring of tumor growth, Anal. Biochem. 423 (2012) 277–285.
[36] B. Kavosi, A. Salimi, R. Hallaj, K. Amani, A highly sensitive prostate-specific antigen immunosensor based on gold nanoparticles/PAMAM dendrimer loaded on MWCNTS/chitosan/ionic liquid nanocomposite, Biosens. Bioelectron. 52 (2014) 20–28.
[37] B. Demirbakan, M.K. Sezgintürk, A sensitive and disposable indium tin oxide based electrochemical immunosensor for label-free detection of MAGE-1, Talanta 169 (2017) 163–169.
[38] B. Özcan, M.K. Sezgintürk, A novel label free immunosensor based on single-use ITO-PET electrodes for detection MAGE1 protein, J. Electroanal. Chem. 792 (2017) 31–38.
[39] Ç.S. Şimşek, M. Teke, M.K. Sezgintürk, An ITO based disposable biosensor for ultrasensitive analysis of retinol binding protein, Electroanalysis 26 (2014) 328–339.
[40] J.S. Daniels, N. Pourmand, Label-free impedance biosensors: opportunities and challenges, Electroanalysis 19 (2007) 1239–1257.
[41] A.D. McNaught, Compendium of Chemical Terminology, Blackwell Science, Oxford, 1997.
[42] A. Chen, B. Shah, Electrochemical sensing and biosensing based on square wave voltammetry, Anal. Methods 5 (2013) 2158–2173.
[43] R.K. Gupta, A. Periyakaruppan, M. Meyyappan, J.E. Koehne, Label-free detection of C-reactive protein using a carbon nanofiber based biosensor, Biosens. Bioelectron. 59 (2014) 112–119.
[44] S. Singal, R.K. Kotnala, Single frequency impedance analysis on reduced graphene oxide screen-printed electrode for biomolecular detection, Appl. Biochem. Biotechnol. 183 (2017) 672–683.
[45] Z. Liu, W. Li, G.-C. Han, S. Yuan, Z. Chen, Towards label-free impedance biosensors: CRP probe based on thiol Schiff-nickel complex modified gold nanoparticles, J. Electrochem. Soc. 161 (2014) B75–B80.
[46] T. Songjaroen, R.M. Feeny, M.M. Mensack, W. Laiwattanapaisal, C.S. Henry, Label-free detection of C-reactive protein using an electrochemical DNA immunoassay, Sens. Bio-Sens. Res. 8 (2016) 14–19.
[47] M. Thangamuthu, C. Santschi, O.J.F. Martin, Label-free electrochemical immunoassay for C-reactive protein, Biosensors 8 (2018) 34.
[48] M.N.S. Karaboğa, M.K. Sezgintürk, A novel silanization agent based single used biosensing system: detection of C-reactive protein as a potential Alzheimer's disease blood biomarker, J. Pharm. Biomed. Anal. (2018) (DOI).